Acta Pharmaceutica Sinica B 2019;9(3):505–515

Chinese Pharmaceutical Association
Institute of Materia Medica, Chinese Academy of Medical Sciences

Acta Pharmaceutica Sinica B

www.elsevier.com/locate/apsb
www.sciencedirect.com

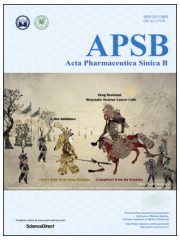

ORIGINAL ARTICLE

Inhibition of FOXO3a/BIM signaling pathway contributes to the protective effect of salvianolic acid A against cerebral ischemia/reperfusion injury

Junke Song[a,b], Wen Zhang[a,b], Jinhua Wang[a,b], Haiguang Yang[a,b], Qimeng Zhou[a,b], Haigang Wang[a,b], Li Li[a,b], Guanhua Du[a,b,*]

[a]*State Key Laboratory of Bioactive Substances and Functions of Natural Medicines, Institute of Materia Medica, Chinese Academy of Medical Sciences and Peking Union Medical College, Beijing 100050, China*
[b]*Beijing Key Laboratory of Drug Target Identification and Drug Screening, Institute of Materia Medica, Chinese Academy of Medical Sciences and Peking Union Medical College, Beijing 100050, China*

Received 13 October 2018; received in revised form 21 December 2018; accepted 7 January 2019

KEY WORDS

Salvianolic acid A;
Ischemia reperfusion;
FOXO3a;
BIM;
Neuroprotection

Abstract Salvianolic acid A (SalA) is an effective compound extracted from traditional Chinese medicine *Salvia miltiorrhiza* Bunge. The Forkhead box O3a (FOXO3a) signaling pathway plays crucial roles in the modulation of ischemia-induced cell apoptosis. However, no information about the regulatory effect of SalA on FoxO3a is available. To explore the anti-cerebral ischemia effect and clarify the therapeutic mechanism of SalA, SH-SY5Y cells and Sprague–Dawley rats were applied, which were exposed to oxygen glucose deprivation/reoxygenation (OGD/R) and middle cerebral artery occlusion/reperfusion (MCAO/R) injuries, respectively. The involved pathway was identified using the specific inhibitor LY294002. Results showed that SalA concentration-dependently inhibited OGD/R injury triggered cell viability loss. SalA reduced cerebral infarction, lowered brain edema, improved neurological function, and inhibited neuron apoptosis in MCAO/R rats, which were attenuated by the treatment of phosphatidylinositol-4,5-bisphosphate 3-kinase (PI3K) specific inhibitor LY294002. SalA time- and concentration-dependently upregulated the phosphorylation levels of protein kinase B (AKT) and its downstream protein FOXO3a. Moreover, the nuclear translocation of FOXO3a was inhibited by SalA

*Corresponding author. Tel./fax: +86 10 63165184.
E-mail address: dugh@imm.ac.cn (Guanhua Du).

Peer review under responsibility of Institute of Materia Medica, Chinese Academy of Medical Sciences and Chinese Pharmaceutical Association.

https://doi.org/10.1016/j.apsb.2019.01.010

both *in vivo* and *in vitro*, which was also reversed by LY294002. The above results indicated that SalA fought against ischemia/reperfusion damage at least partially *via* the AKT/FOXO3a/BIM pathway.

1. Introduction

Stroke is considered to be one of most severe life-threatening diseases with high incidence, high mortality, and high disability worldwide[1,2]. Ischemic stroke accounts for 87% of all stroke types[3,4]. Complicated mechanisms and pathophysiological events have been implicated to involve in ischemic stroke injury including oxidative stress, inflammatory response, calcium overload, excitotoxicity, etc[5]. Besides the Food and Drug Administration (FDA) approved tissue plasminogen activator (tPA), few other therapeutic agents are clinical available throughout the world. In addition, thrombolytic therapy by tPA only benefits a small proportion of clinical patients due to its narrow thrombolysis window and high risk of hemorrhage injury[6,7]. The development of new therapeutic agent is imperative.

The Forkhead box O (FOXO) proteins family is a group of transcription factors, regulating various genes and proteins expression, such as BCL-like protein 11 (BIM) and matrix metalloproteinases (MMP). FOXO family transcription factors, including FOXO1, 3, 4, and 6, are reported to be the important downstream proteins of phosphatidylinositol-4,5-bisphosphate 3-kinase/protein kinase B (PI3K/AKT) pathway[8–12], one of the most vital regulators in cell survival, autophagy, apoptosis, proliferation and differentiation[13–16]. Kinase in this pathway could phosphorylate Forkhead box O3a (FOXO3a) to induce its redistribution to cytoplasm and reduce its transcriptional activity. FOXO3a has been proved to be a transcriptional target in apoptosis regulation *in vivo* and *in vitro*, which might be a promising target for neuroprotection[8,17].

Salvianolic acid A (SalA) is a polyphenol compound extracted and purified from *Salvia miltiorrhiza* Bunge (Fig. 1A). SalA is one of the major effective components of several traditional Chinese medicine (TCM) preparations for the clinical treatment of cardiovascular and cerebrovascular diseases[18–24]. It was reported that SalA could activate AKT/mammalian target of rapamycin C1 (mTORC1) signaling to initiate NF-E2 related factor 2/heme oxygenase-1 (NRF2/HO-1) signal transduction, thus fighting against H_2O_2-upregulated cellular oxidative stress[25]. SalA pretreatment significantly upregulated the phosphorylation levels of AKT in ischemia/reperfusion injured diabetic rats[26]. SalA alleviated ischemic brain injury in mice partially through the activation of PI3K/AKT signaling[27]. Thus, SalA might activate PI3K/AKT signaling during ischemic injury. But whether SalA could regulate FOXO3a/BIM-induced cell apoptosis was unknown. This work was designed to research the potential therapeutic effect of SalA on oxygen glucose deprivation/reoxygenation (OGD/R)-injured SH-SY5Y cells, as well as on middle cerebral artery occlusion/reperfusion (MCAO/R)-injured rat brain, and especially to find out whether FOXO3a/BIM pathway was involved in the neuroprotective mechanism of SalA.

2. Materials and methods

2.1. Reagents and chemicals

SalA (HPLC purity >99%) was obtained from Institute of Materia Medica, Chinese Academy of Medical Sciences & Peking Union

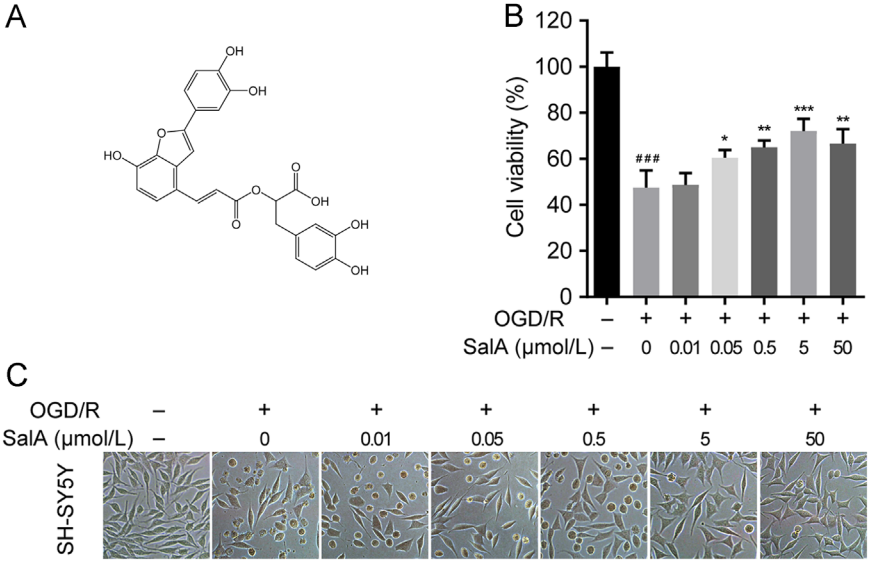

Figure 1 Chemical structure of SalA (A) and its protective effect against OGD/R-induced SH-SY5Y cells viability loss (B) and (C). Cell morphology was obtained by an inverted microscope. Data was expressed as mean ± SD of 4 independent tests. $^{###}P<0.001$ compared with the control group, $^{*}P<0.05$, $^{**}P<0.01$ and $^{***}P<0.001$ compared with the OGD/R group.

Medical College (CAMS & PUMC, Beijing, China). Dulbecco's modified Eagle's medium: Nutrient Mixture F-12 (DMEM/F-12) medium, fetal bovine serum (FBS) and protein marker were obtained from Thermo Fisher Scientific (Waltham, MA, USA). Hoechst 33258, DAPI, 2,3,5-triphenyltetrazolium chloride (TTC) and 3-[4,5-dimehyl-2-thiazolyl]-2,5-diphenyl-2*H*-tetrazolium bromide (MTT) were purchased from Sigma–Aldrich (St. Louis, MO, USA). LY294002 was purchased from Beyotime Institute of Biotechnology (Shanghai, China). Antibodies against FOXO3a, AKT, mammalian target of rapamycin (mTOR), glycogen synthase kinase 3β (GSK3β), p-FOXO3a, p-AKT, p-mTOR, p-GSK3β, BIM, cleaved caspase 3, GAPDH, Lamin B1, FOXO3a siRNA, anti-rabbit IgG (H+L), F(ab′)2 fragment (Alexa Fluor® 488 conjugate) and anti-mouse IgG (H+L), F(ab′)2 fragment (Alexa Fluor® 594 conjugate) were purchased from Cell Signaling Technology (Danvers, MA, USA). Antibody against neuron-specific nuclear protein (NeuN) and glucose transporter 1 (GLUT1) were purchased from Abcam (Cambridge, UK). TUNEL apoptosis detection kit was purchased from Roche (Mannheim, Germany). HRP conjugated goat anti-mouse IgG, HRP conjugated goat anti-rabbit IgG and enhanced chemiluminescence (ECL) Western blot kit were purchased from CWBIO (Beijing, China). Deionized water was prepared *via* a Milli Q Water Purification system from Millipore (Bedford, MA, USA). Other reagents and chemicals were purchased from Beijing Chemical Reagents Co. (Beijing, China).

2.2. SH-SY5Y cell culture

SH-SY5Y cells (China Infrastructure of Cell Line Resources) were cultured in DMEM/F-12 medium supplemented with 10% FBS, 100 μg/mL streptomycin and 100 U/mL penicillin. Cell culture was carried out at 37 °C. The culture condition was maintained at 95% air and 5% CO_2 with a humidified atmosphere. The medium was scheduled renewed every 48 h.

2.3. Oxygen glucose deprivation/reoxygenation and grouping

For OGD stimulation, the culture medium of SH-SY5Y cells was replaced with Earle's balanced salt solution (EBSS, containing 116 mmol/L NaCl, 1 mmol/L NaH_2PO_4, 0.8 mmol/L $MgSO_4$, 0.9 mmol/L $CaCl_2$, 5.4 mmol/L KCl and 10 mg/L phenol red). After medium replacement, cells were immediately transferred into a hypoxic incubator with 94% N_2, 5% CO_2 and 1% O_2 (Thermo Scientific). After OGD injury for 2 h, full culture medium was applied again in the absence or presence of SalA for another 24 h. The experiment was divided into normal control group (culture medium only), OGD/R model group, SalA low concentration group (OGD/R+0.05 μmol/L SalA), SalA middle concentration group (OGD/R+0.5 μmol/L SalA), SalA high concentration group (OGD/R+5 μmol/L SalA), LY294002 pretreatment group (OGD/R+5 μmol/L SalA+10 μmol/L LY294002), control siRNA group (OGD/R+control siRNA) and FOXO3a siRNA group (OGD/R+FOXO3a siRNA) and SalA+FOXO3a group (OGD/R+5 μmol/L SalA+FOXO3a siRNA). LY294002 (10 μmol/L) were pre-treated for 2 h before OGD/R stimulation, and SalA was added and treated for 24 h after OGD/R stimulation with continued LY294002 exposure. For siRNA interference, SH-SY5Y cells were seeded in 6-well plates. After 24 h, 0.8 mL siRNA transfection medium was added to each well. After incubated with FOXO3a siRNA or control siRNA for 6 h, the normal culture medium was added again before OGD/R stimulation.

2.4. MTT assay

Firstly, SH-SY5Y cells were seeded and cultured in 96-well culture plates with 8×10^3 cells per well. After the above mentioned OGD/R injury and SalA treatment procedure, MTT method was carried out to test cell viability. Shortly, each well was added with 0.5 mg/mL MTT reagent, and then incubated at 37 °C for 4 h. Then, remove the cell culture supernatant, and add 100 μL of DMSO to each well. Stir the plate for 15 min on a microplate shaker. Finally, determine the absorbance value of each well by a microplate reader at 490 nm. The cell viability of each well was calculated according to the measured absorbance value.

2.5. Establishment of animal model and grouping

Sprague–Dawley rats (male, 240–260 g) were purchased from Beijing Vital River Experimental Animal Co., Ltd. (Beijing, China; certificate No. SCXK2016-0006). Great efforts have been given to minimize the experiment-induced discomfort and the physical and emotional pain of rats. All the animal related procedures were reviewed and approved for further research by the Institutional Animal Care and Use Committee of the Institute of Materia Medica, CAMS & PUMC (Beijing, China). The MCAO/R model was established according to the method previously reported[28]. Isoflurane was used to anesthetize the rats. After fixed in a supine position, rats underwent the surgery to reveal the right common carotid artery (CCA), external carotid artery (ECA), as well as the internal carotid artery (ICA). Then a filament with a diameter of 0.2 mm was inlet from ECA of rat into ICA and finally got to MCA. After 1.5 h of ischemia, the monofilament was carefully pulled out to achieve cerebral reperfusion. Animals were randomly grouped as follows: sham operation group, I/R model group, I/R+SalA groups (5, 10 and 20 mg/kg) and I/R+SalA+LY294002 group (20 mg/kg SalA and LY294002), $n=40$ for each group. LY294002 was dissolved in 4% DMSO+30% PEG 300+5% Tween 80+ddH_2O to a final concentration of 10 mmol/L. 10 μL LY294002 (10 mmol/L) was pre-injected into the ventricular space of the ischemic hemisphere 1 h before ischemia as mentioned before[29]. SalA was dissolved in normal saline. After the reperfusion, rats were injected intravenously with vehicle or SalA twice a day for 3 days. The followed tests were performed on the fourth day after the reperfusion.

2.6. Neurological deficit scores

Neurological deficit scores evaluation was used for functional assessment. Rat neurological function was tested by an investigator who was blinded to the grouping with a five-point evaluation method as mentioned before[30]. Rats with no observed neurological deficit got a score of 0; rats unable to fully extend left forepaw got a score of 1; rats that circled to left got a score of 2; rats that fell to left got a score of 3; rats unable to walk spontaneously and with depressed levels of consciousness got a score of 4. The rats with a score of 0 point indicating no neurological deficit were screened out of the further study. And the rats with a score of 4 point indicating extremely severe damage were also excluded from the further study.

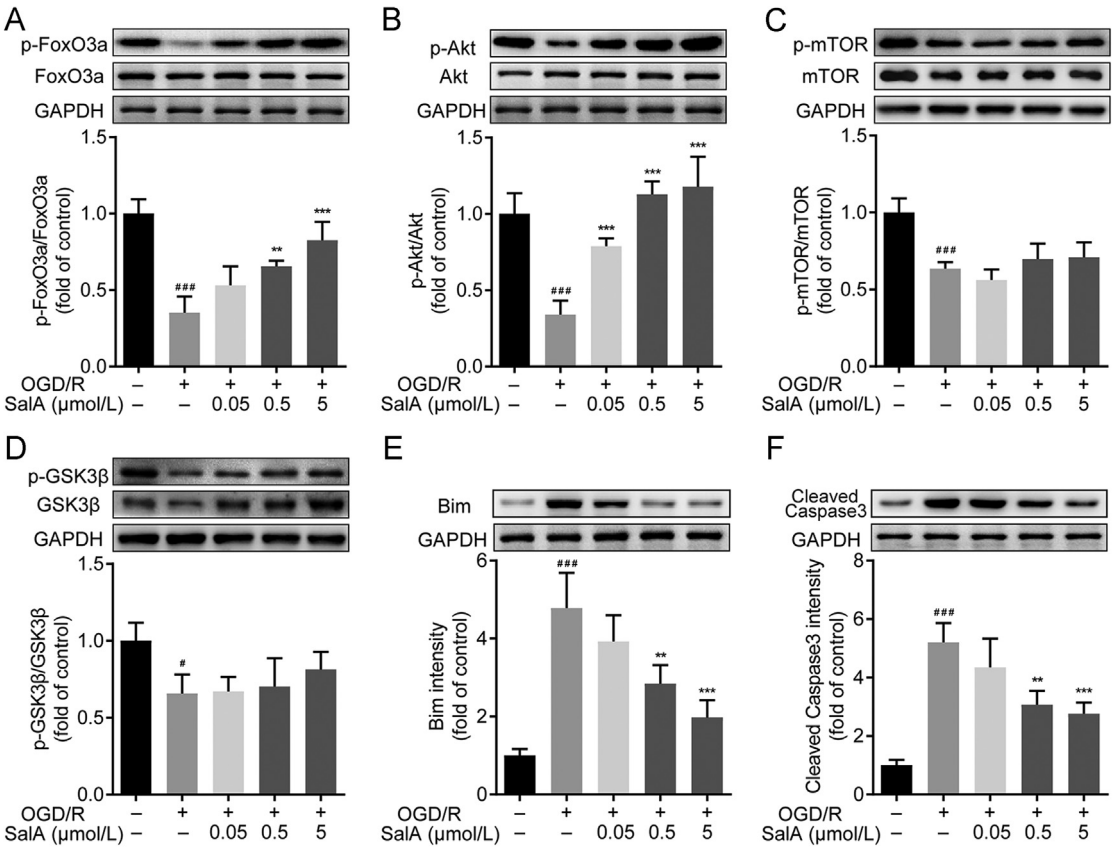

Figure 2 SalA increased AKT and FOXO3a phosphorylation, inhibited BIM and cleaved caspase 3 expression in OGD/R-injured SH-SY5Y cells. (A) The p-FOXO3a/FOXO3a ratio. (B) The p-AKT/AKT ratio. (C) The p-mTOR/mTOR ratio. (D) The p-GSK3β/ GSK3β ratio. (E) The expression of BIM. (F) The expression of cleaved caspase 3. Proteins were analyzed using Western blot method normalized to GAPDH. Data was expressed as mean $\pm$ SD of 4 independent tests. $^{\#}P<0.05$ and $^{\#\#\#}P<0.001$ compared with control group, $^{**}P<0.01$ and $^{***}P<0.001$ compared with OGD/R group.

2.7. *Determination of infarct volume by TTC staining*

Cerebral infarct volume is an important evaluation factor for the efficacy of anti-cerebral ischemia reperfusion drug. In brief, rats were sacrificed after the evaluation of neurological function. The rat brain was separated quickly and placed in a freezer at –20 °C. After 20 min, the brain tissue was taken out at room temperature and dissected into slices of 2-mm thickness. Then slices were quickly placed into TTC solution (0.5%) to react for 30 min, flipped every 5 min, and finally fixed with 4% paraformaldehyde. As a result, the normal area in slice was rose-red, while the infarct area was white without staining. Brain slices of each rat were arranged neatly and photographed. A researcher who was blinded to the rats grouping outlined and calculated the infarct areas and whole areas using ImageJ software (Version 1.51, National Institutes of Health; Bethesda, MA, USA). The infarct volume was calculated by multiplying the infarct area and the thickness (2 mm) of each slice and displayed as a percentage of whole brain volume.

2.8. *Immunofluorescence assay*

The FOXO3a nuclear translocation *in vitro* was observed *via* immunofluorescence assay. After OGD/R stimulation and SalA treatment, cells for fluorescence imaging were fixed using 4% paraformaldehyde. And then they were permeabilized using 0.3% Triton X-100. After blocked by 5% BSA, the primary antibody against FOXO3a was added and incubated at 4 °C overnight. Then Alexa Fluor-488 (1:500)-conjugated secondary antibody was added and incubated for 1 h. Finally, Hoechst 33258 was added and incubated for 30 min. The fluorescent images for the observation of nuclear translocation were taken under a microscope.

The brain tissue for frozen sections was placed in a 4% paraformaldehyde solution and fixed. After that, frozen sections were prepared into 5 μm thickness. For TUNEL and NeuN or GLUT1 double-labeled staining. Proteinase K was firstly incubated. Then the buffer solution, reaction solution, saline sodium citrate, 0.5% Triton X-100 and 10% goat serum were added following steps and incubated as planned. Then cells were treated with primary antibody against NeuN or GLUT1 overnight, and the secondary antibody for 1 h. The fluorescent images of TUNEL were taken under a microscope.

For FOXO3a and NeuN staining, brain slices were firstly treated with 0.5% Triton X-100, and then treated with 10% goat serum. The primary antibodies against FOXO3a and NeuN were then used and reacted overnight. Then the secondary antibodies were used and reacted. Finally, after DAPI treatment, the fluorescent images of FOXO3a and NeuN staining were taken under a microscope.

2.9. *Western blot analysis*

SH-SY5Y cells or brain tissues were both extracted using RIPA buffer. The rat cortex and hippocampus were carefully and rapidly

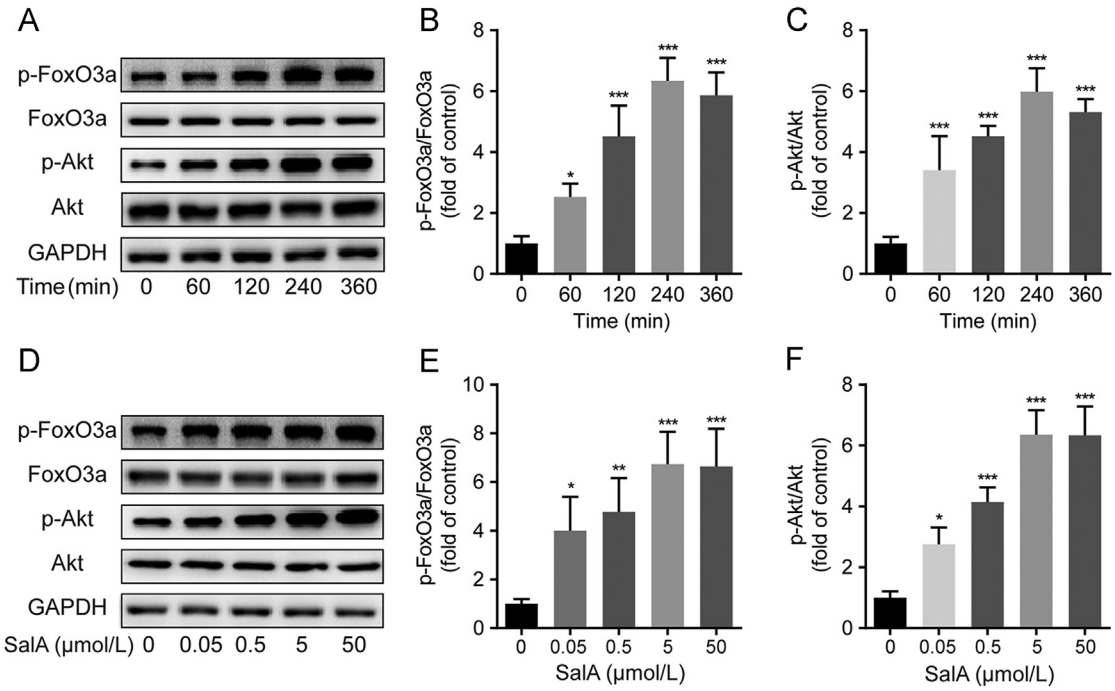

Figure 3 SalA increased the phosphorylation levels of AKT and FOXO3a in a time- and concentration-dependent manner. (A) The levels of p-FOXO3a, FOXO3a, p-AKT and AKT in SH-SY5Y cells treated without or with SalA (5 μmol/L) for 60, 120, 240 and 360 min. (B) The p-FOXO3a/FOXO3a ratio in SH-SY5Y cells treated without or with SalA (5 μmol/L) for 60, 120, 240 and 360 min. (C) The p-AKT/AKT ratio in SH-SY5Y cells treated without or with SalA (5 μmol/L) for 60, 120, 240 and 360 min. (D) The levels of p-FOXO3a, FOXO3a, p-AKT and AKT in SH-SY5Y cells treated without or with SalA (0.05, 0.5, 5 and 50 μmol/L) for 240 min. (E) The p-FOXO3a/FOXO3a ratio in SH-SY5Y cells treated without or with SalA (0.05, 0.5, 5 and 50 μmol/L) for 240 min. (F) The p-AKT/AKT ratio in SH-SY5Y cells treated without or with SalA (0.05, 0.5, 5 and 50 μmol/L) for 240 min. Proteins were analyzed using Western blot method normalized to GAPDH. Data was expressed as mean ± SD of 4 independent tests. $^{*}P<0.05$, $^{**}P<0.01$ and $^{***}P<0.001$ compared with the control group.

separated from brains on ice. Each 0.1 g tissue was added with 1 mL RIPA buffer and homogenized. The homogenate was then lysed on ice for 30 min. A BCA protein assay kit was used for the protein quantification. Proteins were loaded and separated using SDS-PAGE method, then transferred onto a PVDF membrane. After being blocked with 5% BSA for 2 h, proteins were treated with primary antibodies against p-FOXO3a, FOXO3a, p-AKT, AKT, BIM, cleaved caspase 3 and GAPDH at 4 °C overnight. Then the secondary antibodies against HRP-conjugated rabbit or mouse IgG were added to the system. An ECL method was used for image developing. Band density was calculated with the ImageJ software.

2.10. Statistical analysis

The results were shown as mean ± standard deviation (SD). SPSS software (version 16.0, Chicago, IL, USA) was used for data analysis. The significance between groups was carried out by one-way ANOVA analysis followed by Tukey's Multiple Comparison *post hoc* test. A P value <0.05 was calculated to be statistically significant.

3. Results

3.1. Effect of SalA on OGD/R-induced SH-SY5Y cells viability loss

OGD/R stimulation resulted in severe cell damage and cell viability loss ($P<0.001$), while SalA treatment significantly inhibited OGD/R-induced SH-SY5Y cells viability loss at the concentration range of 0.05–5 μmol/L in a concentration dependent manner as shown in the MTT assay and under the inverted microscope. The *in vitro* concentration 5 μmol/L showed maximal neuroprotection effect and was selected for further study.

3.2. SalA increased Akt and FOXO3a phosphorylation, inhibited BIM and cleaved caspase 3 expression in vitro

FOXO3a signaling participates in cell apoptosis regulation. As shown in Fig. 2, OGD/R injury downregulated the phosphorylation levels of AKT and FOXO3a significantly ($P<0.001$). SalA treatment (0.5 and 5 μmol/L) inhibited the downregulation of FOXO3a phosphorylation ($P<0.01$ and $P<0.001$). OGD/R stimulation downregulated the ratios of p-mTOR/mTOR and p-GSK3β/GSK3β. But SalA could not upregulate both ratios of p-mTOR/mTOR and p-GSK3β/GSK3β. So, further studies were focused on the regulation of p-FOXO3a/FOXO3a induced by SalA. Meanwhile, the phosphorylation levels of AKT were upregulated by SalA treatment (0.05, 0.5 and 5 μmol/L). In addition, OGD/R injury significantly upregulated the expression of BIM and cleaved caspase 3 ($P<0.001$), and SalA treatment (0.5 and 5 μmol/L) downregulated the expression of BIM and cleaved caspase 3.

3.3. SalA increased AKT and FOXO3a phosphorylation in a time- and concentration-dependent manner

The above results indicated PI3K/AKT and FOXO3a signaling might mainly contribute to the protective effect of SalA on cells

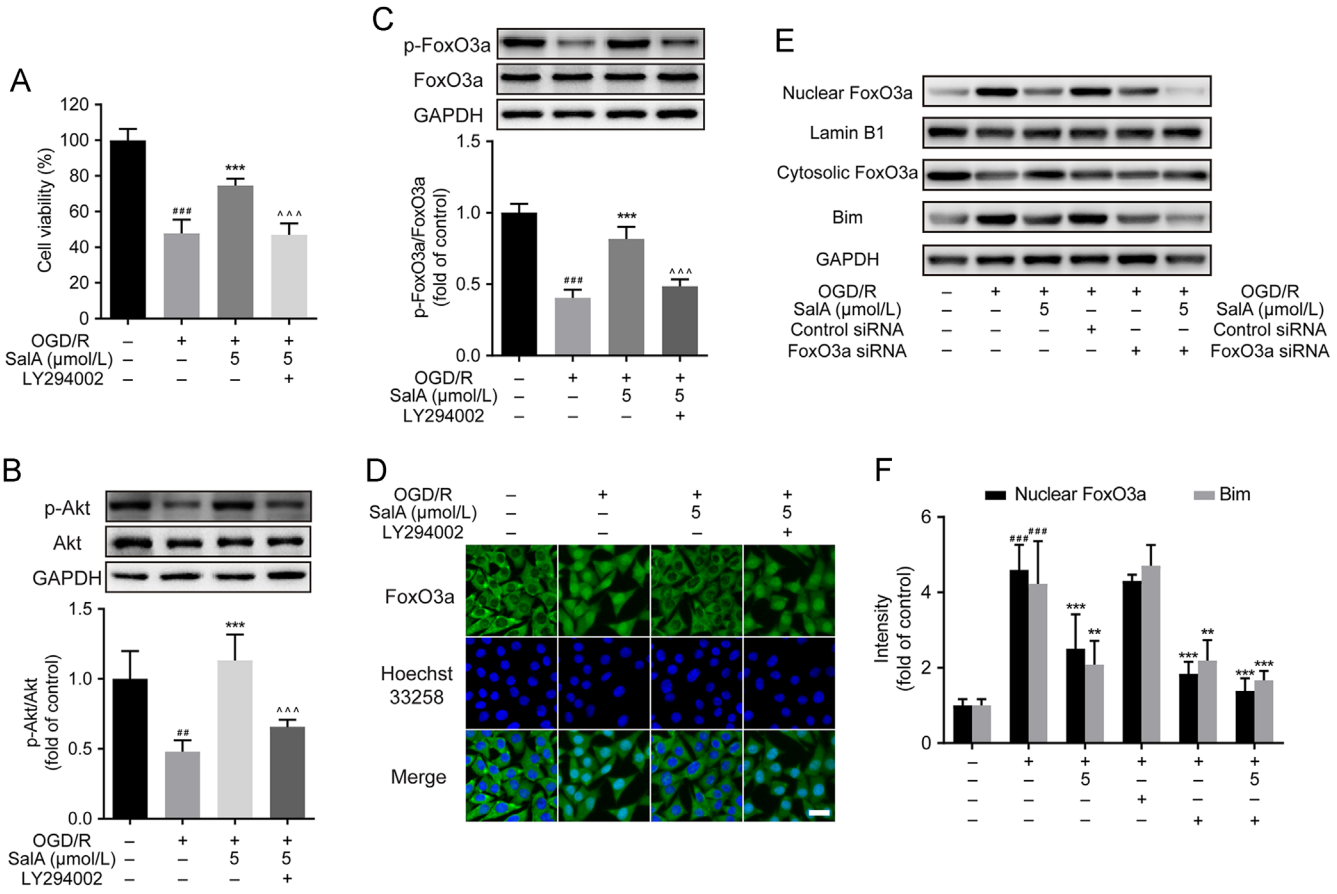

Figure 4 LY294002 reversed SalA-induced cell protective effect, and the AKT and FOXO3a phosphorylation effect *in vitro*. Cells were pre-treated with LY294002 (10 μmol/L) before OGD/R stimulation and SalA treatment. (A) Effects of LY294002 on the protective effects of SalA by MTT assay. (B) The p-AKT/AKT ratio in SH-SY5Y cells treated without or with LY294002 by Western blot assay. (C) The p-FOXO3a/FOXO3a ratio in SH-SY5Y cells treated without or with LY294002 by Western blot assay. (D) The expression and intracellular localization of FOXO3a (green fluorescence) were assessed by immunofluorescence assay. (E) and (F) The nuclear FOXO3a, cytosolic FOXO3a and BIM levels treated without or with FOXO3a siRNA by Western blot assay. Data was expressed as mean ± SD of 4 independent tests. $^{\#\#}P<0.01$ and $^{\#\#\#}P<0.001$ compared with control group, $^{**}P<0.01$ and $^{***}P<0.001$ compared with OGD/R group, $^{\wedge\wedge\wedge}P<0.001$ compared with OGD/R+SalA group. Scale bar = 20 μm.

viability. To confirm the phosphorylation effects of SalA on AKT and FOXO3a, 5 μmol/L concentration of SalA was added and incubated for 60, 120, 240 and 360 min. And 0.05, 0.5, 5 and 50 μmol/L concentrations of SalA were added and incubated for 240 min. Results showed that SalA treatment could increase the phosphorylation levels of AKT and FOXO3a in SH-SY5Y cells in a time- and concentration-dependent manner (Fig. 3).

3.4. SalA activated FOXO3a/BIM signaling through AKT pathway

The above studies indicated that SalA could upregulated the phosphorylation levels of AKT and FOXO3a in SH-SY5Y cells. To find out whether PI3K/AKT contributed to SalA-induced FOXO3a phosphorylation, LY294002 was used. Firstly, cells were pre-treated with LY294002 (10 μmol/L) for 30 min before subjected to OGD/R stimulation and SalA treatment. Then the MTT assay was carried out. The pre-incubation of LY294002 significantly reversed the protective effects of SalA on cell viability (Fig. 4A, $P<0.001$). In addition, pre-incubation with LY294002 significantly reversed SalA-induced AKT phosphorylation, as well as FOXO3a phosphorylation (Fig. 4B and C, $P<0.001$). As shown in Fig. 4D, SalA treatment inhibited the nuclear translocation of FOXO3a, which could be reversed by the interference of LY294002. To evidence FOXO3a/BIM pathway by interfering FOXO3a, FOXO3a siRNA was introduced. It was found that the nuclear FOXO3a level was significantly downregulated by siRNA interference, which triggered the downregulated expression of BIM protein (Fig. 4E and F). These results indicated that PI3K/AKT pathway mainly contributed to the protective effects of SalA and SalA-induced FOXO3a phosphorylation in SH-SY5Y cells. The phosphorylation of FOXO3a reduced the nuclear FOXO3a level, which further resulted in the downregulation of BIM.

3.5. SalA inhibited MCAO/R injury-induced FOXO3a nuclear translocation and upregulated AKT phosphorylation in ischemic rat brain cortex and hippocampus

I/R injury downregulated the cortex phosphorylation levels of AKT and FOXO3a (Fig. 5A–C), while SalA treatment (20 mg/kg) significantly increased the phosphorylation level of FOXO3a ($P<0.01$). In addition, the phosphorylation of AKT was also upregulated by SalA treatment ($P<0.01$) in MCAO/R rats. The

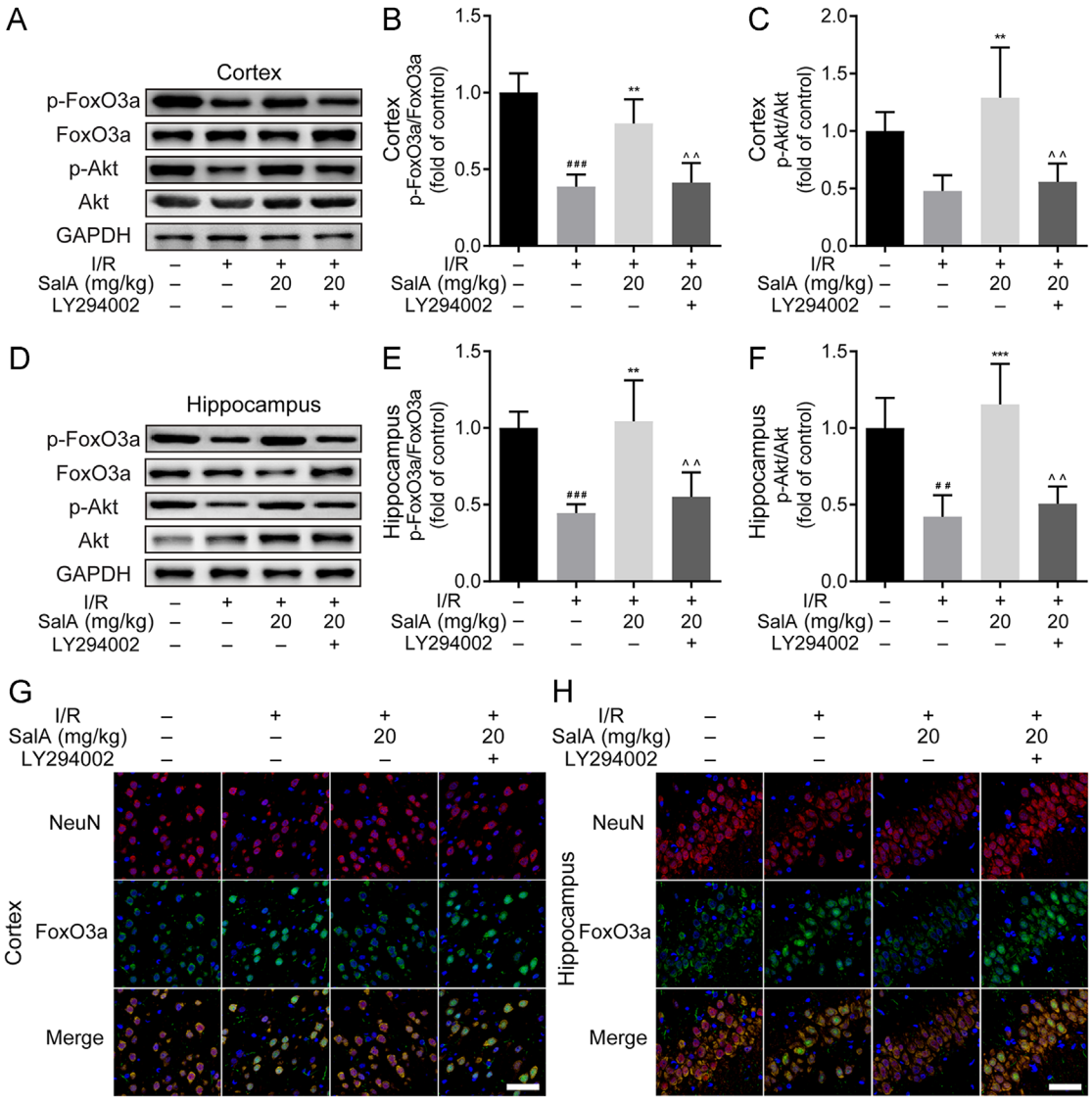

Figure 5 SalA inhibited MCAO/R injury induced FOXO3a nuclear translocation and upregulated AKT phosphorylation in rat brain cortex and hippocampus. (A) The levels of p-FOXO3a, FOXO3a, p-AKT and AKT in rat brain cortex treated by SalA without or with LY294002. (B) The p-FOXO3a/FOXO3a ratio in rat brain cortex treated by SalA without or with LY294002. (C) The p-AKT/AKT ratio in rat brain cortex treated by SalA without or with LY294002. (D) The levels of p-FOXO3a, FOXO3a, p-AKT and AKT in rat brain hippocampus treated by SalA without or with LY294002. (E) The p-FoxO3a/FoxO3a ratio in rat brain hippocampus treated by SalA without or with LY294002. (F) The p-AKT/AKT ratio in rat brain hippocampus treated by SalA without or with LY294002. (G) The expression and localization of FOXO3a (green fluorescence) and NeuN (red fluorescence) in rat brain cortex treated by SalA without or with LY294002 by immunofluorescence assay. (H) The expression and localization of FOXO3a (green fluorescence) and NeuN (red fluorescence) in rat brain hippocampus treated by SalA without or with LY294002 by immunofluorescence assay. Data was expressed as mean ± SD of 4 independent tests. $^{\#\#}P<0.01$ and $^{\#\#\#}P<0.001$ compared with sham group, $^{**}P<0.01$ and $^{***}P<0.001$ compared with I/R group, $^{\wedge\wedge}P<0.01$ compared with I/R+SalA group. Scale bar = 50 μm.

upregulated phosphorylation of FOXO3a and AKT was reversed by LY294002 interference ($P<0.01$) in the brain cortex region. MCAO/R injury also downregulated the levels of p-AKT and p-FOXO3a in the rat brain hippocampus region (Fig. 5D–F). SalA treatment (20 mg/kg) could significantly upregulate the phosphorylation level of FOXO3a in the hippocampus. The phosphorylation level of AKT was also upregulated by SalA treatment in MCAO/R rat hippocampus region. But the upregulated phosphorylation of FOXO3a and AKT was reversed by LY294002 interference in the hippocampus ($P<0.01$). Immunofluorescence assay further verified that SalA treatment inhibited the nuclear translocation of FOXO3a both in the brain cortex and hippocampus regions, which was reversed by the interference of LY294002 (Fig. 5G and H).

3.6. SalA inhibited BIM and cleaved caspase 3 expression in rat brain cortex and hippocampus subjected to MCAO/R injury

MCAO/R injury significantly upregulated the expression of BIM and cleaved caspase 3 in both rat brain cortex and hippocampus (Fig. 6, $P<0.001$), while SalA treatment significantly inhibited the expression of BIM and cleaved caspase 3 in the brain cortex and hippocampus.

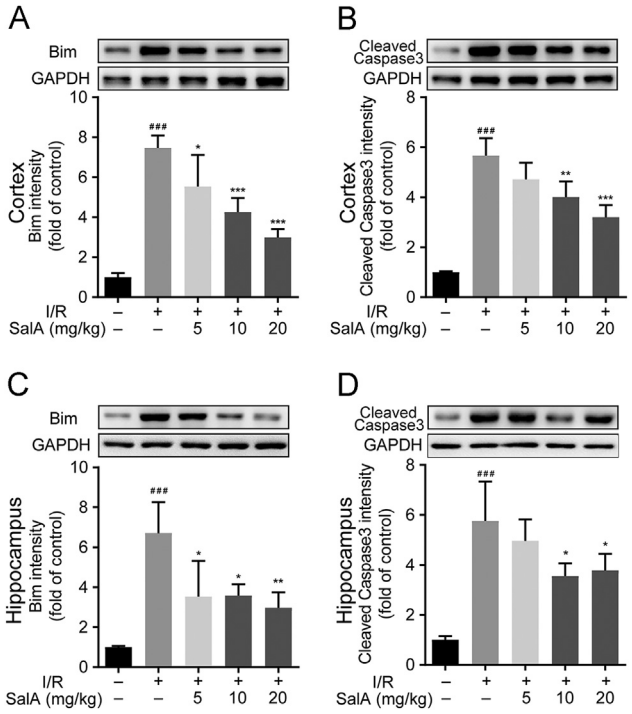

Figure 6 SalA inhibited BIM and cleaved caspase 3 expression in rat brain cortex and hippocampus subjected to MCAO/R injury. (A) The expression of BIM in rat brain cortex treated by SalA. (B) The expression of cleaved caspase 3 in rat brain cortex treated by SalA. (C) The expression of BIM in rat brain hippocampus treated by SalA. (D) The expression of cleaved caspase 3 in rat brain hippocampus treated by SalA. Proteins were analyzed by Western blot assay normalized to GAPDH. Data was expressed as mean ± SD of 4 independent tests. $^{###}P<0.001$ compared with sham group, $^{*}P<0.05$, $^{**}P<0.01$ and $^{***}P<0.001$ compared with I/R group.

3.7. SalA reduced infarct volume, neurological deficit scores, and inhibited neuron and endothelial cells apoptosis in MCAO/R rats

TUNEL staining showed cell apoptosis rate. MCAO/R injury increased the apoptosis rate of neurons in the rat brain cortex ($P<0.001$), SalA treatment (20 mg/kg) decreased neuron apoptosis rate compared with MCAO/R group in cortex, while LY294002 treatment reversed the apoptosis inhibition effects of SalA (Fig. 7A and B). Fig. 7C and D showed that MCAO/R injury also significantly upregulated the neuron apoptosis rate in the rat brain hippocampus region ($P<0.001$), SalA treatment (20 mg/kg) reduced neuron apoptosis compared with MCAO/R group in the hippocampus, which was also reversed by LY294002 treatment. Fig. 7E and F showed that MCAO/R injury significantly upregulated the apoptosis rate of GLUT1 positive cells in the rat brain ischemic penumbra region ($P<0.001$), SalA treatment (20 mg/kg) significantly inhibited GLUT1 positive cells apoptosis compared with MCAO/R group, which was also reversed by LY294002 treatment.

TTC staining was used to assess brain infarction. As shown in Fig. 7G and H, there was almost no infarction in sham group, MCAO/R group developed severe infarction ($P<0.001$). SalA decreased the percent of infarct volume significantly ($P<0.001$). LY294002 partially reversed the downregulation effects of SalA on brain infarction ($P<0.001$). Neurological deficit scores were assessed on the fourth day after reperfusion. MCAO/R caused severe neurological impairment compared with sham operation group ($P<0.001$). SalA (20 mg/kg) reduced the neurological deficit scores significantly ($P<0.001$). And LY294002 also reversed the effects of SalA on neurological deficit scores ($P<0.01$).

4. Discussion

In the present study, it was found that SalA treatment significantly protected SH-SY5Y cells against OGD/R-induced cell death and fought against I/R injury in SD rats. The protective effects of SalA were achieved *via* the inhibition of the FOXO3a/BIM pathway, which further inhibited cell apoptosis. This was the first study to reveal that the neuroprotective effect of SalA was at least partially related to its regulation on FOXO3a/BIM pathway.

The FOXO family of proteins plays key roles in cell growth, development, differentiation, metabolism and apoptosis[31]. FOXO3a has three sites (T32, S253, and S315) with strongest evidence of being phosphorylated by Akt[32]. According to previous studies, PI3K/AKT is involved in the defense against cerebral ischemia-reperfusion injury[33,34]. FOXO3a could be phosphorylated by the PI3K/AKT pathway[35]. The phosphorylation of FOXO3a blocks its nuclear localization and reduces the transcription of the target genes. Once translocated into the nucleus, FOXO3a could bind to *Bim* promoter to promote BIM protein expression, thus initiating the apoptosis pathway[36]. The specific mechanism of SalA on FOXO3a/BIM signaling has not yet been clarified before. Therefore, studies were carried both *in vivo* and in *vitro* to investigate whether SalA can participate in the protective effect against I/R injury through the FOXO3a/BIM signaling pathway. SH-SH5Y cells were used to establish OGD/R stimulation model *in vitro*. The protective mechanism of SalA on neurons was proved by MTT assay. It was found that SalA protected cells from OGD/R injury *via* increasing cell viability. BCL-2 protein family plays key role in apoptosis regulation and serves as the major regulator of mitochondrial function and the release of apoptotic factors[37,38]. BIM is an important member of BH3-only BCL-2 family[39]. It is an important pro-apoptotic protein[40,41]. The pro-apoptotic activity is controlled by both transcriptional regulation and post-translational modification[42,43]. SalA could promote the phosphorylation of FOXO3a and reduce the expression of pro-apoptotic protein BIM.

To clarify the role of AKT/FOXO3a/BIM signaling in neuroprotection, the specific inhibitor LY294002 was investigated. The experimental results showed that the protective effects of SalA *in vitro* could be reversed by LY294002 treatment, and the SalA-induced upregulation of p-AKT and p-FOXO3a were also been inhibited significantly. The phosphorylation of FOXO3a leaded to the change of its cellular localization. OGD/R stimulation reduced the phosphorylation of FOXO3a, facilitating its translocation into the nucleus. SalA could inhibit the nuclear translocation of FOXO3a, while LY294002 reversed the effects of SalA to keep FOXO3a in the nucleus. What's more, the protective effect of SalA on cell viability was also reversed by the treatment of the PI3K inhibitor LY294002. FOXO3a siRNA interference also significantly downregulated the nuclear FOXO3a level, which triggered the downregulated expression of BIM protein. Taken together, the PI3K/AKT/FOXO3a/BIM pathway is confirmed to participate in the protective mechanism of SalA against OGD/R injury.

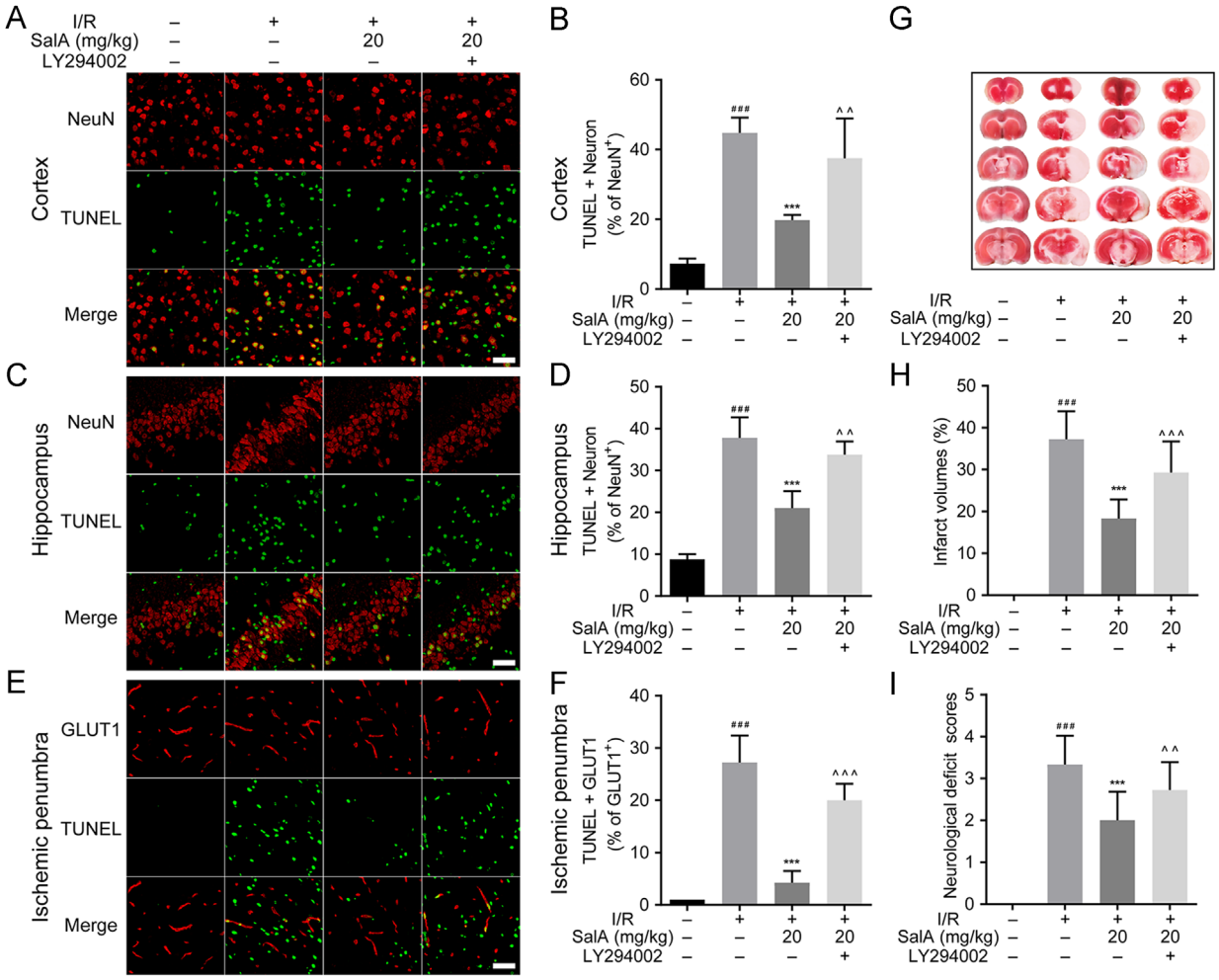

Figure 7 SalA reduced infarct volume, neurological deficit scores, and inhibited neuron and endothelial cells apoptosis in MCAO/R rats. (A) TUNEL and NeuN staining of cortex region. (B) The percent of TUNEL+NeuN positive cells of total neurons in cortex region. (C) TUNEL and NeuN staining of hippocampus region. (D) The percent of TUNEL+NeuN positive cells of total neurons in the hippocampus region. (E) TUNEL and GLUT1 staining of ischemic penumbra region. (F) The percent of TUNEL+GLUT1 positive cells of total GLUT1 positive cells in the ischemic penumbra region. (G) TTC staining of brain slices. (H) Percent of infarct volume calculated according to the thickness of brain slice and the area of infarct region by TTC staining ($n=12$). (I) Neurological deficit scores ($n=18$). $^{\#\#\#}P<0.001$ compared with sham group, $^{***}P<0.001$ compared with I/R group, $^{\wedge\wedge}P<0.01$ and $^{\wedge\wedge\wedge}P<0.001$ compared with I/R+SalA group. Scale bar=50 μm.

Our previous study found that SalA alleviated renal injury through anti-inflammation in systemic lupus erythematosus induced by pristane in BALB/c mice[44]. SalA could alleviate the ischemic injury *via* the inhibition of soluble epoxide hydrolase[45]. SalA was also found to alleviate mice brain ischemic damage *via* anti-inflammation, anti-apoptosis and promoting neurogenesis[27]. The pharmacokinetic study of SalA showed that it could pass across the blood–brain barrier (BBB) to play the protective effect. It was found that I/R injury caused serious damage to the BBB. The serious damage of BBB facilitated the passage of SalA through BBB to the brain. The brain exposure to SalA was significantly higher in the I/R rats than in the sham controls, suggesting that the enhanced exposure to SalA contributed to its cerebral protective effect. It was found that the peak concentration of SalA in brain after 10 mg/kg injection was about 1.5 μg/mL[46]. In our paper, 20 mg/kg SalA was applied, the peak concentration of SalA in brain was supposed to be about 3 μg/mL. That means the 5 μmol/L concentration (2.47 μg/mL for unit conversion) *in vitro* could be reached at the target site *in vivo* if 20 mg/kg SalA is applied. In our present study, SalA was proved to increase the phosphorylation levels of AKT and FOXO3a in both the cortical and hippocampal neurons. The FOXO3a/BIM signaling was proved to be involved in the protective mechanism of many other agents against various injury[11,47,48]. Our study for the first time clarified the regulation effect of SalA on FOXO3a/BIM signaling. The expression of BIM and cleaved caspase 3 were significantly increased by the ischemia reperfusion injury, while SalA treatment downregulated the expression of BIM and cleaved caspase 3. The TUNEL staining results also showed that SalA could reduce the apoptosis rate of neurons, but the above anti-apoptosis effect and FOXO3a phosphorylation effect of SalA on MCAO/R rats were reversed by LY294002 intervene.

In conclusion, our present study reported for the first time that SalA attenuated cerebral ischemia-reperfusion injury at least partially *via* the AKT/FOXO3a/BIM pathway. The regulation of FOXO3a/BIM signaling by SalA suggested a novel promising approach for neuroprotection and provided new insights about the protective mechanism of SalA.

Acknowledgment

This work was supported by grants from National Natural Science Foundation of China (No. 81603100) and the CAMS Innovation Fund for Medical Sciences (2017-I2M-1-010, China).

References

1. Feigin VL, Lawes CM, Bennett DA, Anderson CS. Stroke epidemiology: a review of population-based studies of incidence, prevalence, and case-fatality in the late 20th century. *Lancet Neurol* 2003;**2**:43–53.
2. Feigin VL, Forouzanfar MH, Krishnamurthi R, Mensah GA, Connor M, Bennett DA, et al. Global and regional burden of stroke during 1990–2010: findings from the Global Burden of Disease Study 2010. *Lancet* 2014;**383**:245–54.
3. Benjamin EJ, Blaha MJ, Chiuve SE, Cushman M, Das SR, Deo R, et al. Heart disease and stroke statistics—2017 update: a report from the American Heart Association. *Circulation* 2017;**135**:e146–603.
4. Hlavica M, Diepers M, Garcia-Esperon C, Ineichen BV, Nedeltchev K, Kahles T, et al. Pharmacological recanalization therapy in acute ischemic stroke—evolution, current state and perspectives of intravenous and intra-arterial thrombolysis. *J Neuroradiol* 2015;**42**:30–46.
5. Chamorro Á, Dirnagl U, Urra X, Planas AM. Neuroprotection in acute stroke: targeting excitotoxicity, oxidative and nitrosative stress, and inflammation. *Lancet Neurol* 2016;**15**:869–81.
6. Wang X, Tsuji K, Lee S-R, Ning M, Furie KL, Buchan AM, et al. Mechanisms of hemorrhagic transformation after tissue plasminogen activator reperfusion therapy for ischemic stroke. *Stroke* 2004;**35**:2726–30.
7. Wardlaw JM, Murray V, Berge E, del Zoppo G, Sandercock P, Lindley RL, et al. Recombinant tissue plasminogen activator for acute ischaemic stroke: an updated systematic review and meta-analysis. *Lancet* 2012;**379**:2364–72.
8. Liu MH, Yuan C, He J, Tan TP, Wu SJ, Fu HY, et al. Resveratrol protects PC12 cells from high glucose-induced neurotoxicity *via* PI3K/Akt/FoxO3a pathway. *Cell Mol Neurobiol* 2015;**35**:513–22.
9. Yan P, Tang S, Zhang H, Guo Y, Zeng Z, Wen Q. Palmitic acid triggers cell apoptosis in RGC-5 retinal ganglion cells through the Akt/FoxO1 signaling pathway. *Metab Brain Dis* 2017;**32**:453–60.
10. Zeng B, Li Y, Niu B, Wang X, Cheng Y, Zhou Z, et al. Involvement of PI3K/Akt/FoxO3a and PKA/CREB signaling pathways in the protective effect of fluoxetine against corticosterone-induced cytotoxicity in PC12 cells. *J Mol Neurosci* 2016;**59**:567–78.
11. Zhang MQ, Zheng YL, Chen H, Tu JF, Shen Y, Guo JP, et al. Sodium tanshinone IIA sulfonate protects rat myocardium against ischemia-reperfusion injury *via* activation of PI3K/Akt/FOXO3A/Bim pathway. *Acta Pharmacol Sin* 2013;**34**:1386–96.
12. Zhang X, Tang N, Hadden TJ, Rishi AK. Akt, FoxO and regulation of apoptosis. *Biochim Biophys Acta* 2011;**1813**:1978–86.
13. Song Z, Han X, Shen L, Zou H, Zhang B, Liu J, et al. PTEN silencing enhances neuronal proliferation and differentiation by activating PI3K/Akt/GSK3beta pathway *in vitro*. *Exp Cell Res* 2018;**363**:179–87.
14. Yu Y, Wu X, Pu J, Luo P, Ma W, Wang J, et al. *Lycium barbarum* polysaccharide protects against oxygen glucose deprivation/reoxygenation-induced apoptosis and autophagic cell death *via* the PI3K/Akt/mTOR signaling pathway in primary cultured hippocampal neurons. *Biochem Biophys Res Commun* 2018;**495**:1187–94.
15. Yang Y, Wang Y, Zhao M, Jia H, Li B, Xing D. Tormentic acid inhibits IL-1β-induced chondrocyte apoptosis by activating the PI3K/Akt signaling pathway. *Mol Med Report* 2018;**17**:4753–8.
16. An H, Duan Y, Wu D, Yip J, Elmadhoun O, Wright JC, et al. Phenothiazines enhance mild hypothermia-induced neuroprotection *via* PI3K/Akt regulation in experimental stroke. *Sci Rep* 2017;**7**:7469.
17. Abd El-Aal SA, Abd El-Fattah MA, El-Abhar HS. CoQ10 augments rosuvastatin neuroprotective effect in a model of global ischemia *via* inhibition of NF-kappaB/JNK3/Bax and activation of Akt/FOXO3A/Bim cues. *Front Pharmacol* 2017;**8**:735.
18. Yunfei L, Haibin Q, Yiyu C. Identification of major constituents in the traditional Chinese medicine "QI-SHEN-YI-QI" dropping pill by high-performance liquid chromatography coupled with diode array detection-electrospray ionization tandem mass spectrometry. *J Pharm Biomed Anal* 2008;**47**:407–12.
19. Li X, Du F, Jia W, Olaleye OE, Xu F, Wang F, et al. Simultaneous determination of eight Danshen polyphenols in rat plasma and its application to a comparative pharmacokinetic study of DanHong injection and Danshen injection. *J Sep Sci* 2017;**40**:1470–81.
20. Xu L, Shen P, Bi Y, Chen J, Xiao Z, Zhang X, et al. Danshen injection ameliorates STZ-induced diabetic nephropathy in association with suppression of oxidative stress, pro-inflammatory factors and fibrosis. *Int Immunopharmacol* 2016;**38**:385–94.
21. Yang M, Orgah J, Zhu J, Fan G, Han J, Wang X, et al. Danhong injection attenuates cardiac injury induced by ischemic and reperfused neuronal cells through regulating arginine vasopressin expression and secretion. *Brain Res* 2016;**1642**:516–23.
22. Wang Y, Gao LN, Cui YL, Jiang HL. Protective effect of danhong injection on acute hepatic failure induced by lipopolysaccharide and D-galactosamine in mice. *Evid Based Complement Altern Med* 2014;**2014**:153902.
23. Wan LM, Tan L, Wang ZR, Liu SX, Wang YL, Liang SY, et al. Preventive and therapeutic effects of Danhong injection on lipopolysaccharide induced acute lung injury in mice. *J Ethnopharmacol* 2013;**149**:352–9.
24. Lian-Niang L, Rui T, Wei-Ming C. Salvianolic acid A, a new depside from roots of *Salvia miltiorrhiza*. *Planta Med* 1984;**50**:227–8.
25. Zhang H, Liu YY, Jiang Q, Li KR, Zhao YX, Cao C, et al. Salvianolic acid A protects RPE cells against oxidative stress through activation of Nrf2/HO-1 signaling. *Free Radic Biol Med* 2014;**69**:219–28.
26. Chen Q, Xu T, Li D, Pan D, Wu P, Luo Y, et al. JNK/PI3K/Akt signaling pathway is involved in myocardial ischemia/reperfusion injury in diabetic rats: effects of salvianolic acid A intervention. *Am J Transl Res* 2016;**8**:2534–48.
27. Chien MY, Chuang CH, Chern CM, Liou KT, Liu DZ, Hou YC, et al. Salvianolic acid A alleviates ischemic brain injury through the inhibition of inflammation and apoptosis and the promotion of neurogenesis in mice. *Free Radic Biol Med* 2016;**99**:508–19.
28. Chopp M, Zhang RL, Chen H, Li Y, Jiang N, Rusche JR. Postischemic administration of an anti-Mac-1 antibody reduces ischemic cell damage after transient middle cerebral artery occlusion in rats. *Stroke* 1994;**25**:869–75.
29. Zhao H, Shimohata T, Wang JQ, Sun G, Schaal DW, Sapolsky RM, et al. Akt contributes to neuroprotection by hypothermia against cerebral ischemia in rats. *J Neurosci* 2005;**25**:9794–806.
30. Longa EZ, Weinstein PR, Carlson S, Cummins R. Reversible middle cerebral artery occlusion without craniectomy in rats. *Stroke* 1989;**20**:84–91.
31. Tia N, Singh AK, Pandey P, Azad CS, Chaudhary P, Gambhir IS. Role of Forkhead Box O (FOXO) transcription factor in aging and diseases. *Gene* 2018;**648**:97–105.
32. Manning BD, Cantley LC. AKT/PKB signaling: navigating downstream. *Cell* 2007;**129**:1261–74.
33. Zhu H, Zhang Y, Shi Z, Lu D, Li T, Ding Y, et al. The neuroprotection of liraglutide against ischaemia-induced apoptosis through the activation of the PI3K/AKT and MAPK pathways. *Sci Rep* 2016;**6**:26859.
34. Yu ZH, Cai M, Xiang J, Zhang ZN, Zhang JS, Song XL, et al. PI3K/Akt pathway contributes to neuroprotective effect of Tongxinluo against focal cerebral ischemia and reperfusion injury in rats. *J Ethnopharmacol* 2016;**181**:8–19.

35. Chen Q, Chen X, Han C, Wang Y, Huang T, Du Y, et al. FGF-2 transcriptionally down-regulates the expression of BNIP3L *via* PI3K/Akt/FoxO3a signaling and inhibits necrosis and mitochondrial dysfunction induced by high concentrations of hydrogen peroxide in H9c2 cells. *Cell Physiol Biochem* 2016;**40**:1678–91.
36. Gilley J, Coffer PJ, Ham J. FOXO transcription factors directly activate *bim* gene expression and promote apoptosis in sympathetic neurons. *J Cell Biol* 2003;**162**:613–22.
37. Aouacheria A, Baghdiguian S, Lamb HM, Huska JD, Pineda FJ, Hardwick JM. Connecting mitochondrial dynamics and life-or-death events *via* Bcl-2 family proteins. *Neurochem Int* 2017;**109**:141–61.
38. Deng J. How to unleash mitochondrial apoptotic blockades to kill cancers?. *Acta Pharm Sin B* 2017;**7**:18–26.
39. Shukla S, Saxena S, Singh BK, Kakkar P. BH3-only protein BIM: an emerging target in chemotherapy. *Eur J Cell Biol* 2017;**96**:728–38.
40. O'Connor L, Strasser A, O'Reilly LA, Hausmann G, Adams JM, Cory S, et al. Bim: a novel member of the Bcl-2 family that promotes apoptosis. *EMBO J* 1998;**17**:384–95.
41. Bouillet P, Purton JF, Godfrey DI, Zhang L-C, Coultas L, Puthalakath H, et al. BH3-only Bcl-2 family member Bim is required for apoptosis of autoreactive thymocytes. *Nature* 2002;**415**:922–6.
42. Seo SU, Woo SM, Min K-j, Kwon TK. Z-FL-COCHO, a cathepsin S inhibitor, enhances oxaliplatin-induced apoptosis through upregulation of Bim expression. *Biochem Biophys Res Commun* 2018;**498**:849–54.
43. Peng H, Du B, Jiang H, Gao J. Over-expression of CHAF1A promotes cell proliferation and apoptosis resistance in glioblastoma cells *via* AKT/FOXO3a/Bim pathway. *Biochem Biophys Res Commun* 2016;**469**:1111–6.
44. Lin YH, Yan Y, Zhang HF, Chen YC, He YY, Wang SB, et al. Salvianolic acid A alleviates renal injury in systemic lupus erythematosus induced by pristane in BALB/c mice. *Acta Pharm Sin B* 2017;**7**:159–66.
45. Wang SB, Pang XB, Zhao Y, Wang YH, Zhang L, Yang XY, et al. Protection of salvianolic acid A on rat brain from ischemic damage *via* soluble epoxide hydrolase inhibition. *J Asian Nat Prod Res* 2012;**14**:1084–92.
46. Feng SQ, Aa N, Geng JL, Huang JQ, Sun RB, Ge C, et al. Pharmacokinetic and metabolomic analyses of the neuroprotective effects of salvianolic acid A in a rat ischemic stroke model. *Acta Pharmacol Sin* 2017;**38**:1435–44.
47. Wang H, Zhou X, Huang J, Mu N, Guo Z, Wen Q, et al. The role of Akt/FoxO3a in the protective effect of venlafaxine against corticosterone-induced cell death in PC12 cells. *Psychopharmacology* 2013;**228**:129–41.
48. Yang C, Cao Y, Zhang Y, Li L, Xu M, Long Y, et al. Cyclic helix B peptide inhibits ischemia reperfusion-induced renal fibrosis *via* the PI3K/Akt/FoxO3a pathway. *J Transl Med* 2015;**13**:355.